



SOME STUDIES ON SUPERPLASTICITY IN A FINE GRAINED AA5083 ALLOY

P. Surya Prakash Rao and S. S. Bhattacharya

*Department of Metallurgical and Materials Engineering
Indian Institute of Technology Madras, Chennai-600036, India.*

ABSTRACT

The aluminium alloy AA5083 has attracted a lot of attention because of its good corrosion resistance, weldability, high strength and the capacity towards superplastic behaviour. The dominant mechanism during superplastic deformation is Grain Boundary Sliding (GBS), concomitant with grain boundary migration and grain rotation¹. In the present study emphasis is placed on the microstructural and surface topographic characterization of superplastically deformed AA5083. Tensile tests were performed at temperatures ranging from 748 K to 823 K at initial strain rates ranging from $1 \times 10^{-4} \text{ s}^{-1}$ to $1 \times 10^{-2} \text{ s}^{-1}$. The alloy exhibited substantial deformation at the conditions of testing. Metallographic and fractographic studies were carried out on the deformed specimens and the results reported.

Keywords: Superplasticity, Grain boundary sliding, Cavitation and Strain rate.

1. INTRODUCTION

There has always been a strong interest in the use of superplastic deformation routes for the fabrication of aerospace and automotive parts, especially from titanium and aluminium alloys. Among the different aluminium alloys used, Al-Mg alloy show considerable promise as lightweight structure materials owing to their low density, high strength, good weldability and superior corrosion resistance.

Recently, a lot of attention has been generated on the superplasticity and superplastic deformation of Al-Mg based alloys. The degree of superplasticity in engineering alloys is strongly influenced by grain size and grain size distribution². During deformation the grains apparently slide past one another without noticeable permanent changes in shape^{1,3}. The major mechanisms involved in superplastic deformation include Grain Boundary Sliding (GBS), grain rotation and Grain Boundary Migration (GBM). Experimental data and recent models indicate that GBS is the dominant deformation process and controls the rate of flow^{4,5}. In this study the superplastic behaviour of a AA5083 alloy was investigated and the analysis of fractured specimens using scanning electron microscopy was carried out.

2. EXPERIMENTAL PROCEDURE

The material used in this study was a modified AA5083 aluminium alloy available in the form of a cold rolled 1.5 mm thick sheet. Specimens (Fig.1) with their longitudinal axis parallel to the rolling direction having gauge dimensions of 12.5 mm length and 4 mm width were used for the high temperature tensile tests at temperatures ranging from 748–823 K (475–550 °C) at 25° intervals. A

microprocessor controlled Schneck-Trebel electro-mechanical testing machine of 250 kN capacity with a two-zone split furnace was used. The machine was interfaced with a computer for data acquisition and processing. Temperature accuracy was within $\pm 3^\circ$. Each sample was held at the testing temperature for about 10 minutes in order to reach thermal equilibrium.

The tensile tests were conducted at different constant Cross Head Speeds (CHS), during which the true strain rate continued to decrease as the specimen elongated. At each temperature, five different initial strain rates, viz., $1.04 \times 10^{-4} \text{ s}^{-1}$, $5.2 \times 10^{-4} \text{ s}^{-1}$, $2.0 \times 10^{-3} \text{ s}^{-1}$, $5.33 \times 10^{-3} \text{ s}^{-1}$ and $1.0 \times 10^{-2} \text{ s}^{-1}$ (corresponding to CHS of $0.078 \text{ mm min}^{-1}$, 0.39 mm min^{-1} , 1.5 mm min^{-1} , 4.0 mm min^{-1} and 7.5 mm min^{-1} respectively) were employed. All the tests were carried out until fracture and the load-elongation data acquired. The true stress (σ_t) and true strain (ϵ_t) values were calculated from the load-elongation data. The fracture surfaces were observed using a Scanning Electron Microscope (SEM).

3. RESULTS AND DISCUSSION

A Transmission Electron Micrograph (TEM) of the as-received material showed equiaxed grains with an average grain size of $8 \mu\text{m}$ (Fig. 2a) and second phase particles of size approximately $0.3 \mu\text{m}$ in length and $0.1 \mu\text{m}$ in width (Fig. 2b). Fig. 3 shows the strain hardening characteristics (in terms of the true stress – true strain plots) of specimens tested at different strain rates at temperatures of 773 K (500°C) and 823 K (550°C). The plots show an increase in the strain to failure with an increase in the initial strain rate of testing. Further, the slope of the stress strain curve also decreases with decreasing initial strain rate, thereby delaying the attainment of maximum stress prior to failure. Extensive strain hardening takes place initially and after reaching maximum, the flow stress decreases continuously until fracture. This could be due to dynamic grain growth and or dislocation structure evolution⁶. At higher deformation rates the strain hardening rate saturates early during deformation whereas the slower deformation rates show a more sustained hardening rate which is maintained to higher strain levels. At high strain rates, the hardening component is essentially due to dislocation processes such as pile-ups, tangles and sub-grain formations⁷, which at the higher temperatures, saturate very quickly. At a lower strain rate of $5.2 \times 10^{-4} \text{ s}^{-1}$, the deformation is almost entirely in the optimal superplastic deformation regime (i.e., by grain boundary sliding as the primary mechanism)¹⁻³.

Steady-state strain hardening was observed in all the cases. Fig. 4 shows the effect of temperature on the true stress at an initial strain rate of $2.0 \times 10^{-3} \text{ s}^{-1}$. Increase in temperature leads to a shift of the peak stress to a higher strain and a reduction in initial work hardening. Localization of plastic deformation resulting in the final necking and fracture was observed in these conditions. At temperatures of 773 K and higher, extensive softening was observed just before failure. Very uniform deformation was observed within the gauge length, with the sample exhibiting superior ductility. At a temperature of 748 K , necking was prevented due to both strain hardening associated with extensive work hardening and strain rate hardening associated with m values greater than 0.4 ^{1,3}.

When a superplastic material fails during tensile deformation it is either the result of unstable plastic flow or a consequence of the growth and interlinkage of internally nucleated voids³. The rate at which the discontinuity in the cross sectional area increases depends on both the rate of strain hardening and the strain rate sensitivity³. Surface observations showed that GBS plays an important role in superplastic deformation at all testing temperatures (Fig. 5). Fig. 6 depicts the fracture surfaces (SEM images) of specimens tested at (a) 823 K at an initial strain rate of $1 \times 10^{-4} \text{ s}^{-1}$ (b) 748

K at an initial strain rate of $2 \times 10^{-3} \text{ s}^{-1}$. These indicate ductile quasi-cleavage fracture⁸. In general cavities nucleate at the grain boundaries and their subsequent growth and coalescence invariably leads to premature failure⁴. Fig. 7 shows the cracks and cavities at different temperatures of deformation.

Grain interface at different magnifications is shown in Fig. 8. This demonstrates the phenomenon of grain boundary delamination or voiding which is frequently observed at the free surface during straining, especially at boundaries which are nearly normal to the tensile axis⁵. From a practical viewpoint, the presence of cavities in superplastically formed components adversely affects their mechanical properties.

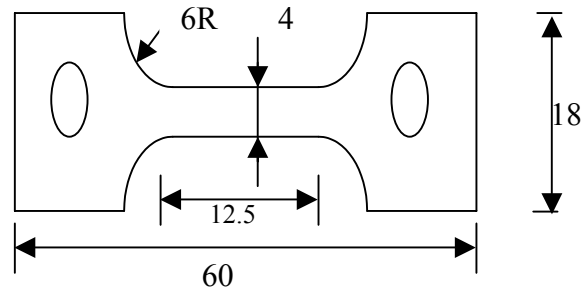
4. CONCLUDING REMARKS

The as-received AA5083 alloy had an average grain size of $8 \mu\text{m}$ with homogeneously distributed second phase particles. Superplastic behaviour of this AA5083 alloy was studied at temperatures ranging from 748 - 823 K and at initial strain rates ranging from $1.04 \times 10^{-4} \text{ s}^{-1}$ to $1.0 \times 10^{-2} \text{ s}^{-1}$. The alloy exhibited good superplastic behaviour in the temperature range of 773-823 K. Extensive strain hardening took place initially and after reaching maximum the flow stress continuously decreased until fracture. Crack propagation along the grain boundary and quasi-cleavage fracture was observed at all test temperatures. Cavitation occurred along the grain boundaries and ultimately led to failure by cavity linked inter granular mode of crack propagation.

5. REFERENCES

1. Padmanabhan K A and Davies G J, *Superplasticity*. Springer-Verlag, Barlin, 1980.
2. Verma R, Ghosh A K, Kim S and Kim C, *Mater. Sci. Eng. A* 191 (1995) 143.
3. Pilling J and Ridley N, *Superplasticity in crystalline solids*, London, The Institute of Metals, 1989.
4. Padmanabhan K A and Schlipf J, *J. Mater. Sci. Tech.*, 12 (1996) 391.
5. Bhattacharya S S, Padmanabhan K A and Schlipf J, *J. Mater. Proc. Manuf. Sci.* 4, (1995) 105.
6. Gifkins R C, *Journal of Materials Science* 13 (1978) 1926.
7. Ravikumar D and Swaminathan K, *Materials at high temperatures* 16(4)(1999) 161.
8. Kaibyshev Oscar A, *Materials Science and Engineering A*, 324 (2002) 96.
9. Surya Prakash Rao P and Bhattacharya S S, *8th International Conference on Non-Ferrous Metals-2004*, Tech-1A/4/1.
10. Wang Y N and Huang J C, *Scripta Materialia* 48(2003) 1117.

FIGURES



All dimensions in mm. (Not to scale)

Fig. 1. High temperature tensile specimen.

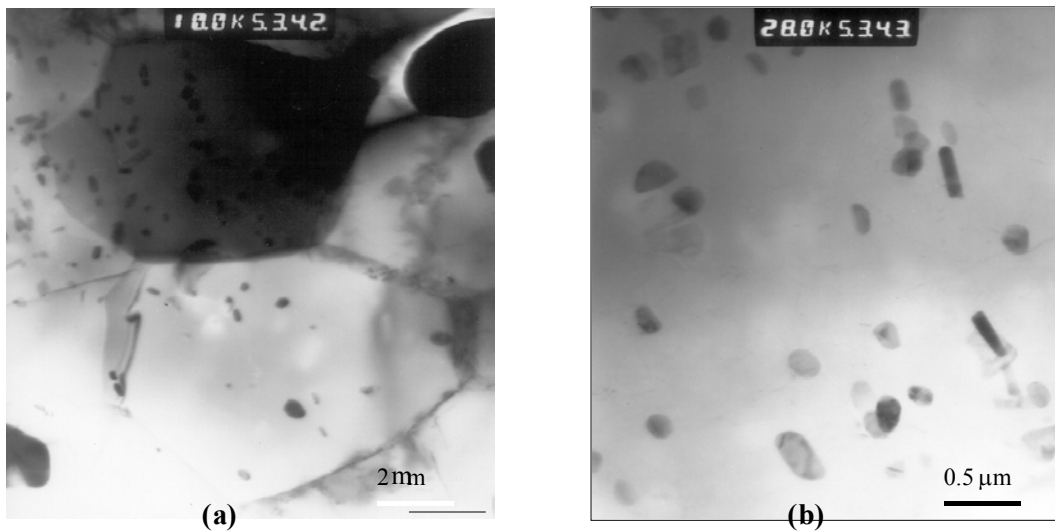


Fig. 2. Transmission electron micrograph of the as received material showing (a) grains and (b) second phase particles.

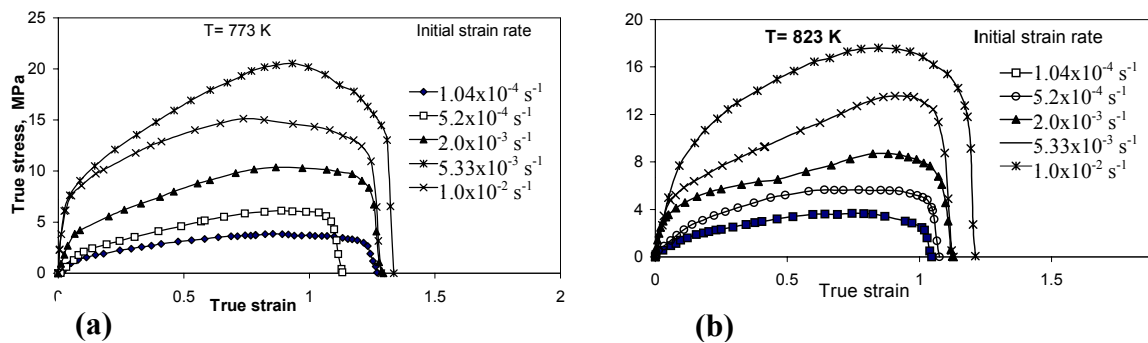


Fig. 3. Effect of the strain rate on the true stress - true strain behaviour at (a) 773 K (b) 823 K.

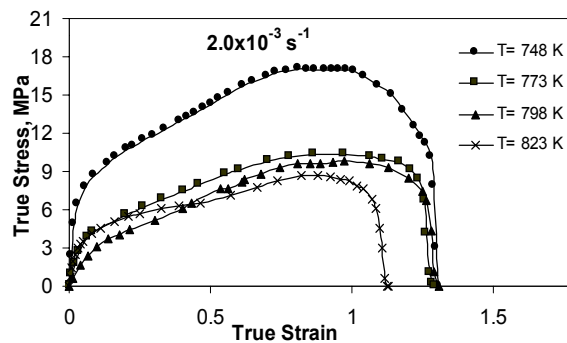


Fig. 4. Effect of temperature on the flow behaviour at an initial strain rate of 2.0x10⁻³ s⁻¹

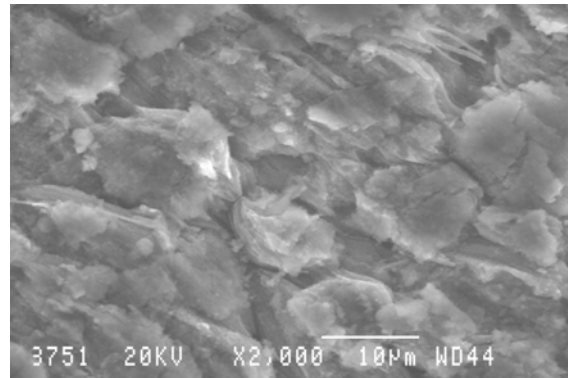


Fig. 5. Surface observations after superplastic deformation at 773 K and an initial strain rate of $1 \times 10^{-2} \text{ s}^{-1}$.

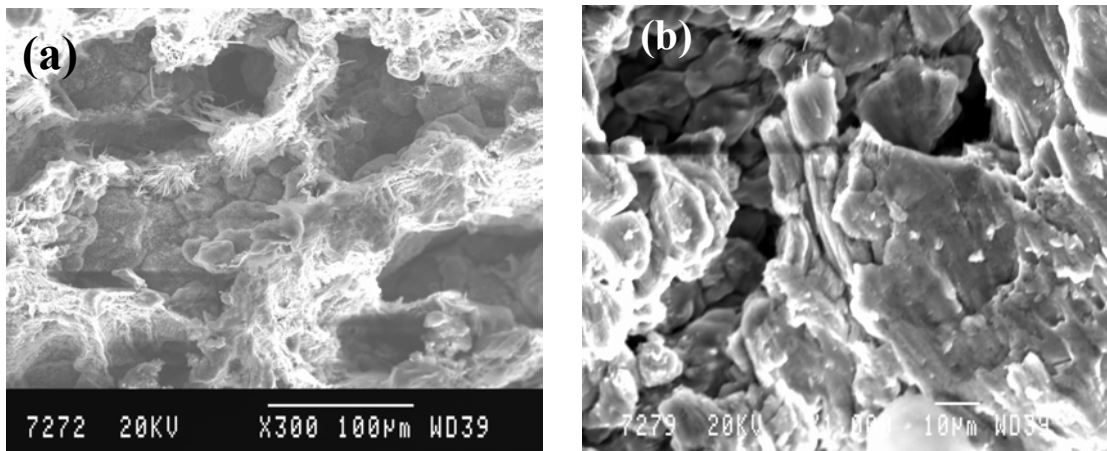


Fig. 6. Fracture surface of specimens tested at (a) 823 K at $1 \times 10^{-4} \text{ s}^{-1}$ initial strain rate and (b) 748 K at $2 \times 10^{-3} \text{ s}^{-1}$ initial strain rate.

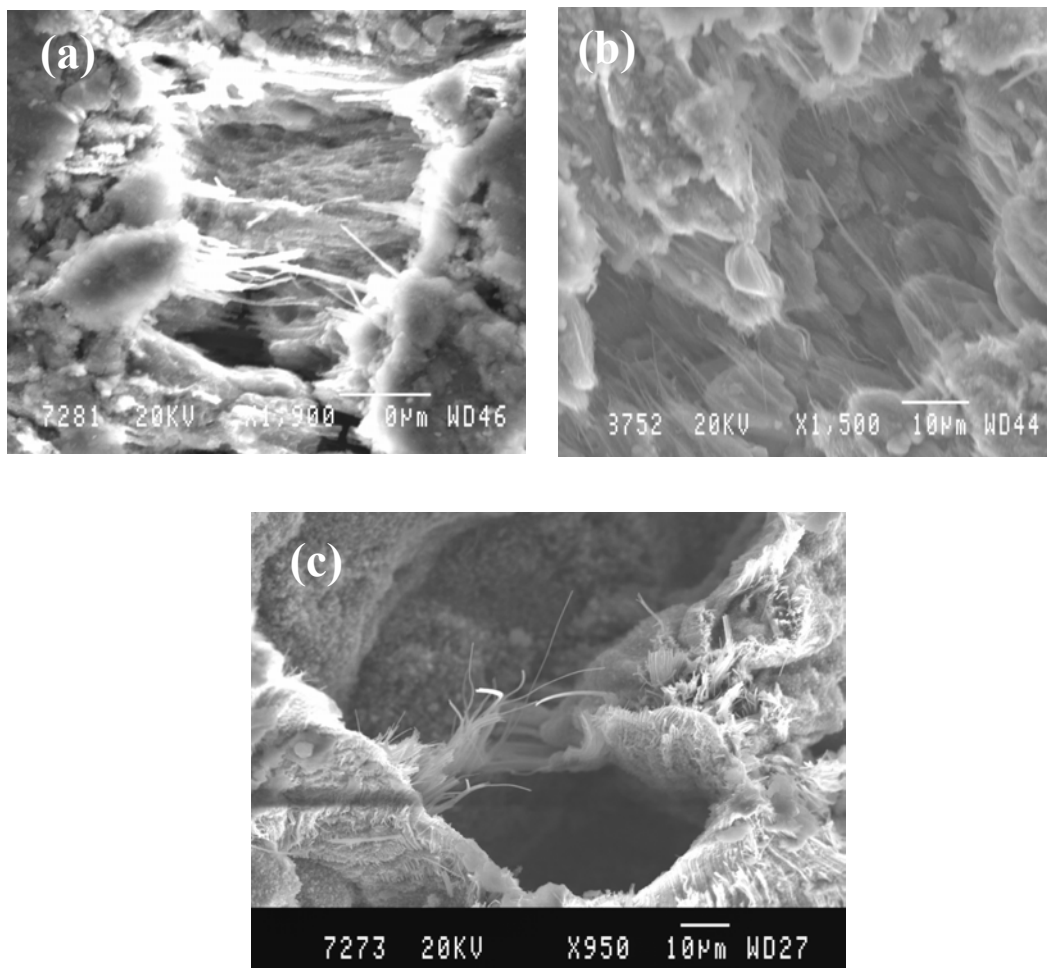


Fig. 7. Fracture surface observations after superplastic deformation at (a) 748 K (b) 773 K and (c) 823 K

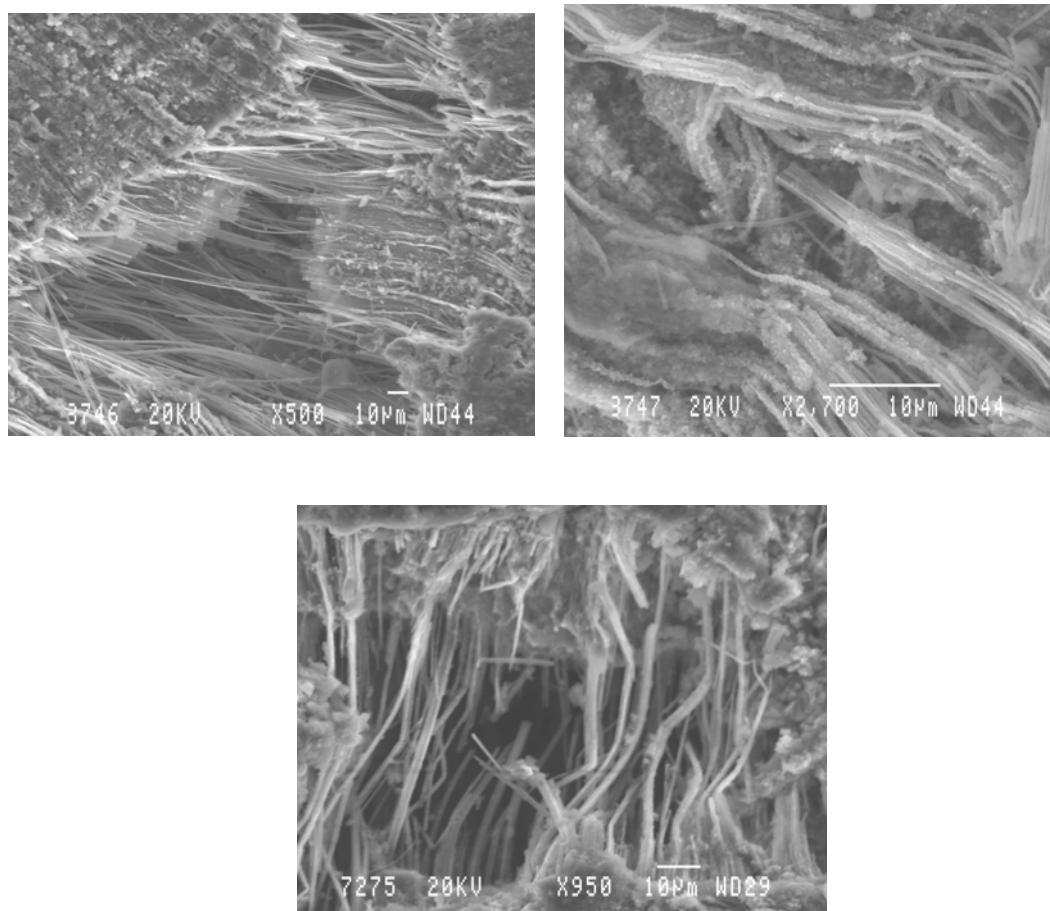


Fig.8. Fractographs of tensile specimens tested at 773 K at different magnifications.